Journal of Enzyme Inhibition and Medicinal Chemistry, 2010; 25(4): 557–564

informa
healthcare

ORIGINAL ARTICLE

Synthesis, characterization, DNA interaction, and cytotoxicity of novel Pd(II) and Pt(II) complexes

Enjun Gao, Fuchun Liu, Mingchang Zhu, Lei Wang, Yun Huang, Hongyan Liu, Shuang Ma, Qunzhi Shi, and Ni Wang

Laboratory of Coordination Chemistry, Shenyang Institute of Chemical Technology, Shenyang, China

Abstract

Four complexes [Pd(L)(bipy)Cl]·4H_2O (1), [Pd(L)(phen)Cl]·4H_2O (2), [Pt(L)(bipy)Cl]·4H_2O (3), and [Pt(L)(phen)Cl]·4H_2O (4), where L = quinolinic acid, bipy = 2,2′-bipyridyl, and phen = 1,10-phenanthroline, have been synthesized and characterized using IR, ^{1}H NMR, elemental analysis, and single-crystal X-ray diffractometry. The binding of the complexes to FS-DNA was investigated by electronic absorption titration and fluorescence spectroscopy. The results indicate that the complexes bind to FS-DNA in an intercalative mode and the intrinsic binding constants K of the title complexes with FS-DNA are about 3.5×10^4 M^{-1}, 3.9×10^4 M^{-1}, 6.1×10^4 M^{-1}, and 1.4×10^5 M^{-1}, respectively. Also, the four complexes bind to DNA with different binding affinities, in descending order: complex 4, complex 3, complex 2, complex 1. Gel electrophoresis assay demonstrated the ability of the Pt(II) complexes to cleave pBR322 plasmid DNA.

Keywords: *Pd(II) and Pt(II) complexes; DNA-binding; cleavage; cytotoxic effect*

Introduction

Cisplatin (cis-diamminedichloroplatinum(II)) is one of the most effective anticancer drugs in the treatment of a variety of human tumors[1,2], and is currently being used clinically. Unfortunately, its usefulness is limited due to the development of resistance in tumor cells and its significant side effects[3]. The search for new metal-based complexes with low toxicity and improved therapeutic properties has attracted considerable attention[4,5]. However, all the research that has involved direct structural analogs of cisplatin have not shown improved clinical efficacy in comparison with the parent drug, most likely because all cis-[PtX_2(amine)$_2$] compounds show similar DNA-binding modes, thereby resulting in similar biological consequences. One approach to overcome this shortcoming is to look past the structure–activity of cisplatin analogs and identify novel materials that can be utilized as building blocks with different DNA-binding modes from that of cisplatin[6,7]. Recently, complexes of the transition metals have been reported to intercalate between DNA base pairs, behaving as artificial DNA nucleases and generating nicks at different DNA sites[8–11]. Furthermore, it is reported that this series of complexes produce significantly more cytotoxic and antiproliferative effects compared with controls[12].

Because of the similar coordination modes and chemical properties of palladium(II) and platinum(II), they both adopt dsp^2 orbital hybridization, forming a square planar complex. Based on the structural analogy between Pt(II) and Pd(II) complexes, the present article includes the synthesis, structural characterization, and preliminary biological activity studies of four complexes of the general formula [M(L)(L_1)Cl]·4H_2O,where L is a quinolinic acid ligand and L_1 is a bipy (bipy = 2,2′-bipyridyl) or phen (phen = 1,10-phenanthroline) ligand (Figure 1).

Materials and methods

All chemicals and reagents purchased were of reagent grade and used without further purification unless otherwise noted. The starting material for synthesis of the title complexes, $K_2[PdCl_4]$, K_2PtCl_4[Potasslum tetrachloroplatinate(II)] was obtained from Sinopharm Chemical Reagent Co.,Ltd., was synthesized by us, and $PdCl_2$, HCl and KCl, quinolinic acid, and 2,2′-bipyridyl were obtained from commercial

Address for Correspondence: Enjun Gao, Laboratory of Coordination Chemistry, Shenyang Institute of Chemical Technology, Shenyang 110142, China. Tel: 86 24 89385016. Fax: 86 24 89388211. E-mail: ejgao@yahoo.com.cn

(Received 20 September 2009; accepted 22 September 2009)

ISSN 1475-6366 print/ISSN 1475-6374 online © 2010 Informa UK Ltd
DOI: 10.3109/14756360903357635

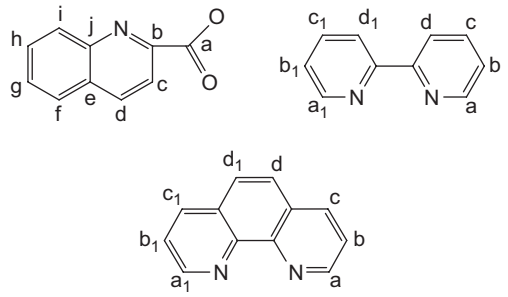

Figure 1. Schematic structure of the ligands and the numbering scheme for ^{1}H NMR spectroscopy.

suppliers. Fish sperm (FS)-DNA and pBR322 plasmid DNA were purchased in China. HeLa (human cervix epitheloid carcinoma) cells, Hep-G2 cells, KB cells, and AGZY-83a (human lung carcinoma) cells were obtained from the American Type Culture Collection.

Synthesis of complexes

The complex [Pd(L)(bipy)Cl]·4H_2O (1) was synthesized as follows. $K_2[PdCl_4]$ (32.6 mg, 0.1 mmol) was dissolved in water (10 mL), and in a separate beaker, ligand L (20.9 mg, 0.1 mmol) was dissolved in water (10 mL). The palladium solution was slowly added dropwise to the solution containing ligand L while stirring, and the mixture was allowed to react for 7 h at room temperature. Then a 10 mL solution of ethanol and water (1:5), containing bipy (2,2′-bipyridyl) (15.6 mg, 0.1 mmol), was added and the mixture was stirred for 6 h under the same conditions. The solution was then filtered and kept in air. Three weeks later, the resulting red-brown crystals were removed, filtered, washed with ether, and dried *in vacuo*. Complex 1 was prepared with a relatively high yield (55.3 mg, 80%). Anal. calcd. (%) for $C_{20}H_{17}ClN_3O_{3.50}Pd$ (1): C, 48.27; H, 3.02; N, 8.45. Found (%): C, 48.05; H, 2.93; N, 8.34; IR (cm^{-1}, s, strong; m, medium; w, weak): ν(O-H) 3420 (m); ν(=C-H) 3081 (w); ν(C=O) 1624 (m); ν(C=C) 1560 (m), 1448 (m); ν(C-N) 1345 (m); ν(C-O) 1169 (w); ν(C-H) 776 (m).^{1}H NMR (DMSO-d_6, 300 MHz): 7.48 (tt, J = 4.8 Hz, 2H, H_b, H_{b1}), 7.82 (t, J = 6.71 H, H, H_h), 7.96 (t, J = 7.5 Hz, 1H, H_i), 7.98 (tt, J = 7.5 Hz, 2H, H_c, H_{c1}), 8.38 (d, J = 7.8 Hz, 1H, H_j), 8.41 (d, J = 7.8 Hz, 1H, H_g), 8.57 (d, J = 8.1 Hz, 1H, H_e), 8.60 (dd, J = 8.1 Hz, 2H, H_a, H_{a1}), 8.69 (d, J = 7.5 Hz, 1H, H_f), 9.13 (dd, J = 4.2 Hz, 2H, H_d, H_{d1}).

The compound [Pd(L)(phen)Cl]·4H_2O (2) was prepared in a similar method as described for 1 with phen (19.8 mg, 0.1 mmol) in place of bipy. The product was obtained as a white powder. Yield: 54.9 mg, 75%. Anal. calcd. (%) for $C_{22}H_{15}N_3O_2PdCl{\cdot}4H_2O$ (2): C, 46.56, H, 4.06, N, 7.41. Found (%): C, 46.45; H, 3.92; N, 7.34; IR (cm^{-1}, s, strong; m, medium; w, weak): ν(O-H) 3391 (m); ν(=C-H) 3037 (w); ν(C=O) 1616 (s); ν(C=C) 1559 (m), 1461 (m); ν(C-N) 1338 (m); ν(C=O) 1253 (w); ν(C-H) 774 (m).^{1}H NMR (DMSO-d_6, 300 MHz): 7.93(t, J = 7.1 Hz, 1H, H_h), 8.07 (tt, J = 8.4 Hz, 2H, H_b, H_{b1}), 8.11 (t, J = 7.5 Hz, 1H, H_i), 8.13 (dd, J = 5.7 Hz, 2H, H_d, H_{d1}), 8.15 (d, J = 8.1 Hz, 1H, H_j), 8.27 (d, J = 7.2 Hz, 1H, H_g), 8.31(d, J = 8.1 Hz, 1H, H_e), 8.96 (tt, J = 7.8 Hz, 2H, H_c, H_{c1}), 8.98 (d, J = 7.8 Hz, 1H, H_f), 9.36 (dd, J = 5.4 Hz, 2H, H_a, H_a).

The compound [Pt(L)(bipy)Cl]·4H_2O (3) was prepared in a similar method as described for 1 with $K_2[PtCl_4]$ (41.5 mg, 0.1 mmol) in place of $K_2[PdCl_4]$. The product was obtained as a yellow powder. Yield: 56.9 mg, 73%. Anal. calcd. (%) for $C_{20}H_{15}N_3O_2PtCl{\cdot}4H_2O$ (3): C, 37.97, H, 3.64, N, 6.65. Found (%): C, 37.88; H, 3.58; N, 6.54; IR (cm^{-1}, s, strong; m, medium; w, weak): ν(O-H) 3440 (m); ν(=C-H) 3078 (w); ν(C=O) 1669 (m); ν(C=C) 1561 (w), 1471 (m); ν(C-N) 1328 (m); ν(C-O) 1243 (w); ν(C-H) 775 (m).^{1}H NMR (DMSO-d_6, 300 MHz): 7.73 (tt, J = 6.9 Hz, 2H, H_b, H_{b1}), 7.85 (t, J = 6.9 Hz, 1H, H_h), 7.98 (t, J = 7.8 Hz, 1H, H_i), 8.12 (tt, J = 6.0 Hz, 2H, H_c, H_{c1}), 8.34 (d, J = 8.4 Hz, 1H, H_j), 8.42 (d, J = 8.1 Hz, 1H, H_g), 8.53 (d, J = 9.3 Hz, 1H, H_e), 8.59 (dd, J = 7.8 Hz, 2H, H_a, H_{a1}), 8.70 (d, J = 4.8 Hz, 1H, H_f), 9.50 (dd, J = 5.7 Hz, 2H, H_d, H_{d1}).

The compound [Pt(L)(phen)Cl]·4H_2O (4) was prepared in a similar method as described for 1 with phen (19.8 mg, 0.1 mmol) in place of bipy. The product was obtained as a red powder. Yield: 55.1 mg, 67%. Anal. calcd. (%) for $C_{22}H_{15}N_3O_2PtCl{\cdot}4H_2O$ (4): C, 40.24, H, 3.51, N, 6.40. Found (%): C, 40.32; H, 3.49; N, 6.34; IR (cm^{-1}, s, strong; m, medium; w, weak): ν(O-H) 3441 (m); ν(=C-H) 3056 (w); ν(C=O) 1670 (m); ν(C=C) 1582 (w), 1460 (w); ν(C-N) 1332 (m); ν(C-O) 1272 (w); ν(C-H) 770 (m).^{1}H NMR (DMSO-d_6, 300 MHz) 7.89(t, J = 6.9 Hz, 1H, H_h), 8.05 (tt, J = 6.3 Hz, 2H, H_b, H_{b1}), 8.11 (t, J = 7.2 Hz, 1H, H_i), 8.14 (dd, J = 5.4 Hz, 2H, H_d, H_{d1}), 8.16 (d, J = 3.0 Hz, 1H, H_j), 8.28 (d, J = 6.6 Hz, 1H, H_g), 8.34 (d, J = 7.8 Hz, 1H, H_e), 8.95 (tt, J = 4.8 Hz, 2H, H_c, H_{c1}), 8.99 (d, J = 8.7 Hz, 1H, H_f), 9.37 (dd, J = 4.8 Hz, 2H, H_a, H_a).

Physical measurements

Elemental analyses were carried out for C, N, and H with a Finnigan EA 1112 model analyzer. Infrared (IR) spectra were run as KBr pellets on a Nicolet IR-470 machine. The ^{1}H nuclear magnetic resosnance (NMR) spectra of dimethylsulfoxide (DMSO) solutions were recorded on a Bruker Avance 300 MHz spectrometer.

Ultraviolet-visible spectra were recorded on a UV-2550 double beam spectrophotometer. Absorption values were determined in the range 200–400 nm, using a 1 cm quartz cuvette. Samples were prepared in buffer (pH 7.4, 50 mM Tris-HCl, 10 mM NaCl) and analyzed at room temperature (20°C).

Fluorescence measurements were obtained on a PerkinElmer LS55 fluorescence spectrofluorometer. For all fluorescence measurements, the entrance and exit slits were both maintained at 10 nm. The sample was excited at 526 nm and its emission appeared at 604 nm. The buffer used in the binding studies was 50 mM Tris-HCl, pH 7.4, containing 10 mM NaCl. The sample was incubated for 4 h at room temperature (20°C) before spectral measurements. Under the experimental conditions, the fluorescence intensity of the respective complexes, FS-DNA, and ethidium bromide was significantly changed. The interaction of the respective

Pd(II) and Pt(II) complexes with DNA *in vitro* was studied as described in the literature[12,13].

For gel electrophoresis experiments, pBR322 plasmid DNA (0.33 μg/μL) was treated with the palladium(II) and platinum(II)complexes. in Tris buffer (50 mM Tris-acetate, 18 mM NaCl buffer, pH 7.2), and the contents were incubated for 1 h at room temperature (20°C). Samples were eletrophoresed for 3 h at 90 V on 0.8% agarose gel in Tris-acetate buffer. After eletrophoresis, the gel was stained with 1 μg/mL ethidium bromide and photographed under UV light.

X-ray crystal structure measurement for complex 1

The crystal structure of complex 1 was determined by singe-crystal X-ray diffraction. A suitable single crystal of dimensions 0.26 × 0.30 × 0.20 mm was mounted in a glass fiber capillary. Crystal data of complex 1 were obtained at 293 K in the range of 2.53° < θ < 26.02°on a Bruker Smart-1000 CCD diffractometer with MoKα radiation (λ = 0.71073). The structure was solved by direct methods using SHELXL-97 software[14] and refined by means of the full-matrix least-squares procedure on F^2 [15]. All non-hydrogen atoms were refined anisotropically. Hydrogen atoms were included at ideal geometric positions. Structure solution and refinement based on 3971 independent reflections with I > 2σ(I) gave R_1 = 0.0383, wR_2 = 0.1193. The CCDC number of this crystal complex 1 is 736056 (unit cell parameters: a 30.151(5), b 13.7611(18), c 9.9804(13), beta 102.449(3), space group C2/c). Crystal data and structure refinement details are summarized in Table 1.

Table 1. Crystal data and refinement for complex 1.

Empirical formula	$C_{20}H_{17}ClN_3O_{3.50}Pd$
Formula weight	497.22
Temperature (K)	293 (2)
Wavelength (Å)	0.71073
Crystal system	Monoclinic
Space group	C2/c
a (Å)	30.151 (5)
b (Å)	13.7611 (18)
c (Å)	9.9804 (13)
α (deg)	90
β (deg)	102.449 (3)
γ (deg)	90
Volume (Å^3)	4043.6 (10)
Z	8
D_{calc} (mg/m^3)	1.633
Absorption coefficient (mm^{-1})	1.078
F(000)	1992
Crystal size	0.29 × 0.15 × 0.07
θ Range for data collection (deg)	2.53–26.02
Index ranges	−31 ≤ h ≤ 37, −16 ≤ k ≤ 16, −11 ≤ l ≤ 12
Reflections collected	11,116
Independent reflections (R_{int})	3971
Data/restraints/parameters	3971/0/275
S	1.026
Final R indices [I > 2σ(I)]	R_1 = 0.0383, wR_2 = 0.1193
R indices (all data)	R_1 = 0.0427, wR_2 = 0.1246
Largest diffraction peak and hole (Å; e^3)	0.903 and −0.577

Cytotoxicity assay

The cytotoxicity of the four complexes was investigated on HeLa cells, Hep-G2 cells, KB cells, and AGZY-83a cells. IC_{50} (the concentration of tested agent that caused 50% inhibition of cell growth) was determined using the MTT assay. This assay is based on cleavage of the yellow tetrazolium salt (3-(4,5-dimethylthiazol-2-yl)-2,5-diphenyl tetrazolium bromide; MTT, Sigma), forming purple formazan crystals by viable cells[16]. The cell lines were grown in 25 cm^2 tissue culture flasks in an incubator at 37°C in a humidified atmosphere consisting of 5% CO_2 and 95% air. The cells were maintained in logarithmic growth phase in complete medium consisting of RPMI 1640, 10% (v/v) heat-inactivated fetal calf serum, 20 mM Hepes, 0.112% bicarbonate, and 2 mM glutamine. In short, the cells were seeded in a 96-well culture plate at 2 × 10^5 cells/well in 100 μL culture medium and 24 h later they were exposed to tested compounds at different concentrations. The cells were incubated for 72 h. Then, 20 μL MTT solution (5 mg/mL) was added to each well and the cells were further cultivated for 4 h. After removal of the medium, DMSO was added to each well to dissolve the formazan crystals, and the absorbance was determined at 450 nm. The IC_{50} values were obtained from the results of quadruplicate determinations of at least three independent experiments.

In another test the effect on cell growth for the four complexes was studied by culturing the cells in medium alone for 1 day, and then treating them for 3 days with 3 μg/mL concentrations. The viable cells remaining at the end of the treatment period were determined by MTT assay and

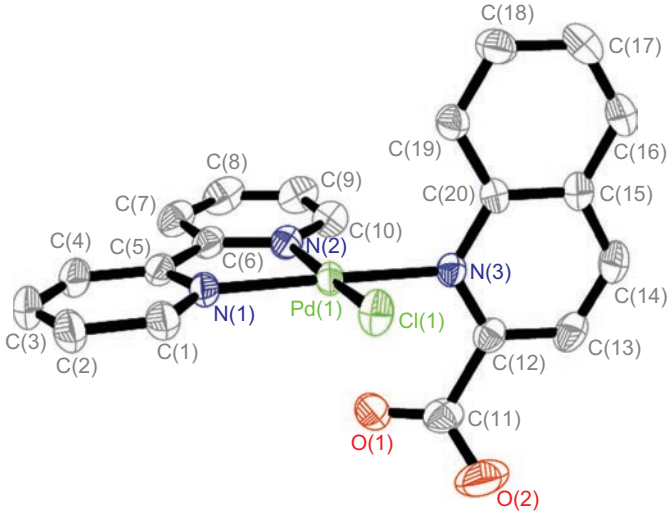

Figure 2. Independent molecule of complex 1 with numbering of atoms (four crystal water and H atoms are omitted for clarity) at 30% probability thermal ellipsoids.

Table 2. Selected bond lengths (Å) and angles (deg) for complex (1).

Pd(1)–N(1)	2.014 (3)	Pd(1)–N(2)	2.021 (3)
Pd(1)–N(3)	2.040 (3)	Pd(1)–Cl(1)	2.2953 (10)
N(1)–Pd(1)–N(2)	80.47 (13)	N(1)–Pd(1)–N(3)	176.03 (12)
N(2)–Pd(1)–N(3)	96.25 (13)	N(1)–Pd(1)–Cl(1)	95.65 (9)
N(2)–Pd(1)–Cl(1)	173.07 (9)	N(3)–Pd(1)–Cl(1)	87.84 (9)
C(1)–N(1)–Pd(1)	125.7 (3)	C(5)–N(1)–Pd(1)	114.5 (3)
C(20)–N(3)–Pd(1)	119.9 (2)	C(6)–N(2)–Pd(1)	114.9 (3)
C(10)–N(2)–Pd(1)	125.6 (3)	C(12)–N(3)–Pd(1)	120.4 (2)

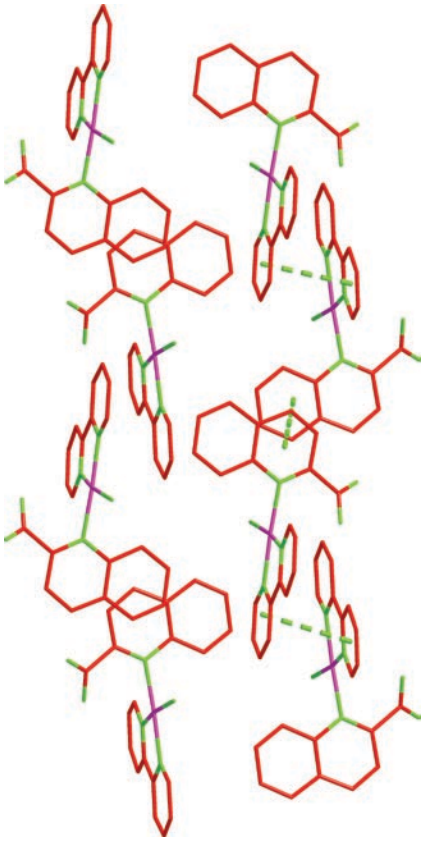

Figure 3. One-dimensional chain of complex 1 through π–π weak interaction (H atoms are omitted for clarity).

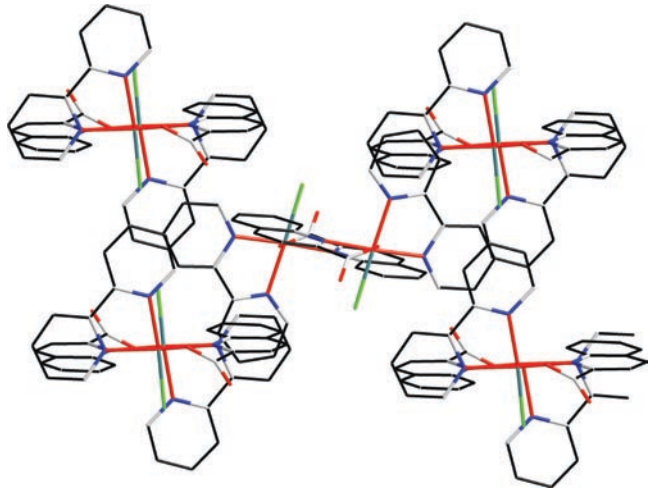

Figure 4. Three-dimensional structure of complex 1 through π–π stacking and CH–π interactions.

calculated as a percentage of control, treated with vehicle alone (DMSO) under similar conditions.

Results and discussion

Crystallographic structure of complex 1

The single-crystal structure of complex 1 was measured by X ray crystallography as shown in Figure 2, and with an atom numbering scheme. Selected bond lengths (Å) and angles (deg) are enumerated in Table 2.

As shown in Figure 2, the palladium atom is coordinated with N(1), N(2), and N(3), which come from the bipy and L ligands, and the Cl from $K_2[PdCl_4]$. In fact, only a few crystal structures have been reported for Pt(NN) complexes[17,18]. Our group has reported crystal structures of the Pd(NN) type complexes[19,20], where NN is phen or bipy, that are analogous to the present complex 1. The N(2)–Pd–Cl angle measures 173.07° and the N(1)–Pd–N(3) angle measures 176.03°, and therefore the coordination geometry of the Pd atom is square planar, with rather small deviations of the ligating atoms from the coordination plane. The plane is determined by four atoms N(1), N(2), C(5), and C(6) from the bipy ligand, and the others consisting of C(12), C(19), C(20), and N(3) from ligand L are almost perpendicular (dihedral angle 85.59°). The L ligands are stacked (centroid-to-centroid distances of 3.639 Å) in an offset face-to-face mode arrangement with a dihedral angle of 11.07°, conforming to an approximate interaction[21]. Through the π–π weak interaction, a one-dimensional chain is constructed, as shown in Figure 3. In Figure 3, there are also CH–π interactions. In the CH–π interactions of the complex, the distance from the closest hydrogen to the plane of the phenyl ring is 2.890. The three-dimensional structure of complex 1 through π–π stacking and CH–π interactions is shown in Figure 4.

Electronic absorption titration

The electronic absorption spectrum is one of the most important means for determining DNA binding of metal complexes[22–24]. The absorption spectra of the four complexes in the absence and presence of FS-DNA are illustrated in Figure 5. In the UV region, the complexes exhibit two intense absorption bands around 230 nm and 275 nm,

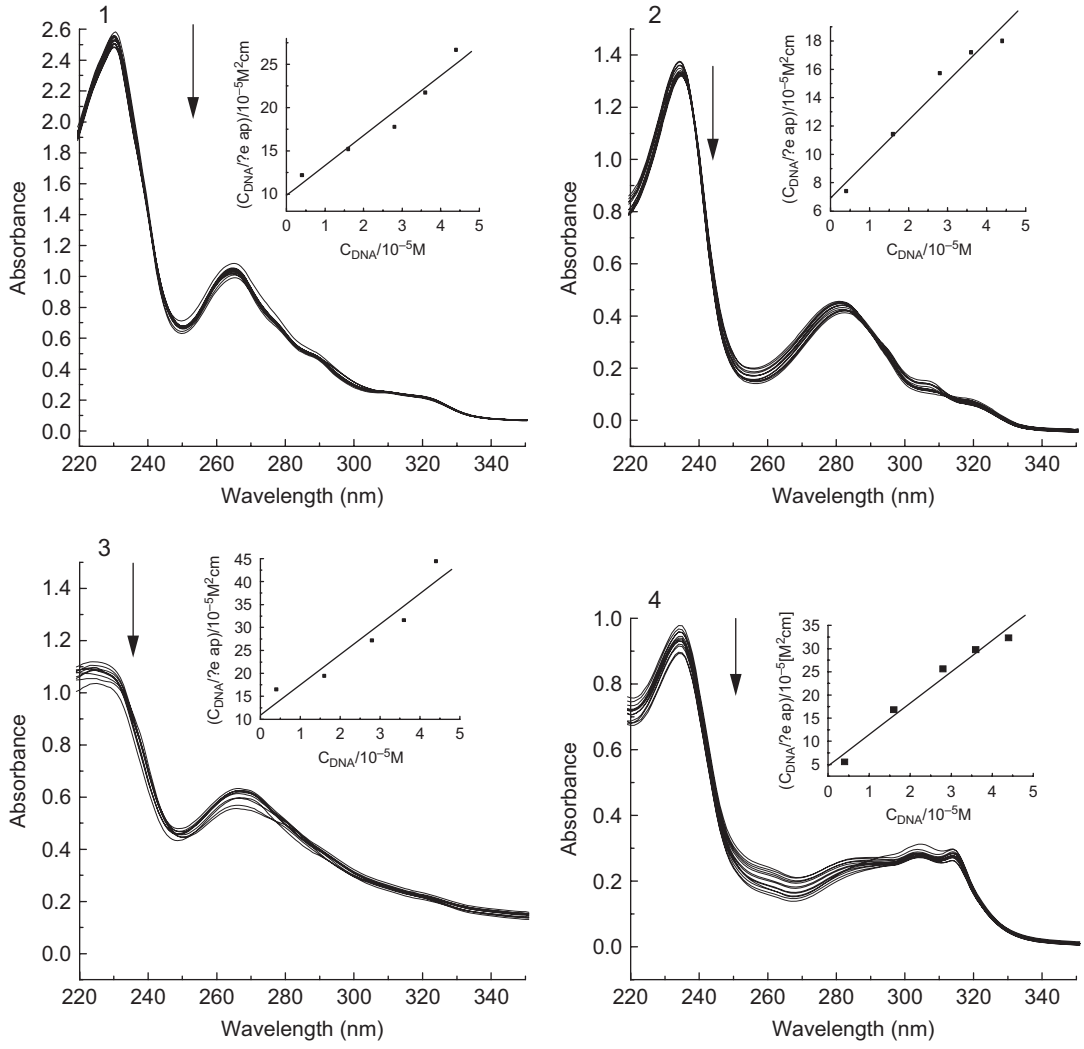

Figure 5. Absorption spectra of four complexes 1, 2, 3, and 4 in the absence and presence of increasing amounts of FS-DNA ([complex] = 10 μM, [DNA] = 0–48 μM). Arrow shows absorbance changes upon increasing DNA concentration. Insets: plots of [DNA]/(εa – εf) versus [DNA] for titration of DNA with the four complexes.

respectively. These absorption bands are attributed to the π–π* transition of the L and bipy ligands[25]. With increasing concentration of FS-DNA, the absorption bands of the complexes are affected, resulting in the slight tendency of reduction in absorbency and red shift. The finding indicates a strong stacking interaction between the aromatic group and the base pairs of FS-DNA, when the complexes intercalate to the FS-DNA. For determining the enucleating action instance between the four complexes and FS-DNA, the intrinsic binding constant K_b of the title complex with FS-DNA was calculated according to the following equation[26], through a plot of [DNA]/(εa – εf) versus [DNA]: [DNA]/(εa – εf) = [DNA]/(εb – εf) + 1/K(εb – εf). Intrinsic binding constants K_b of the four complexes were calculated to be about 3.5×10^4 M^{-1}, 3.9×10^4 M^{-1}, 6.1×10^4 M^{-1}, and 1.4×10^5 M^{-1}, respectively. These K_b values are much smaller than those reported for typical classical intercalators (EtBr–DNA, 3.3×10^5 M^{-1} in 50 mM Tris-HCl/1.0 M NaCl buffer, pH 7.5)[27]. The results are indicative of a weaker binding of DNA with the complexes than with the classical intercalators. It is reasonable to speculate that interaction is comparatively strong between the complexes and FS-DNA.

Fluorescence spectroscopic studies

Fluorescence quenching measurements can be used to investigate metal binding[28]. Ethidium bromide (EtBr) emits intense fluorescence in the presence of DNA due to its strong intercalation between the adjacent DNA base pairs. It has been reported that the enhanced fluorescence can be quenched by the addition of another molecule[29,30], and quenching of DNA–EtBr fluorescence by the addition of complexes causes a reduction in the emission intensity, indicating competition between the complex and EtBr in binding to DNA[31]. The emission spectra of EtBr bound to DNA in the absence and presence of the four complexes are shown in Figure 6. The addition of each Pd(II) and Pt(II) complex to DNA pretreated with EtBr results in an appreciable reduction in fluorescence intensity, denoting that the complexes compete with EtBr to bind with DNA. This is in

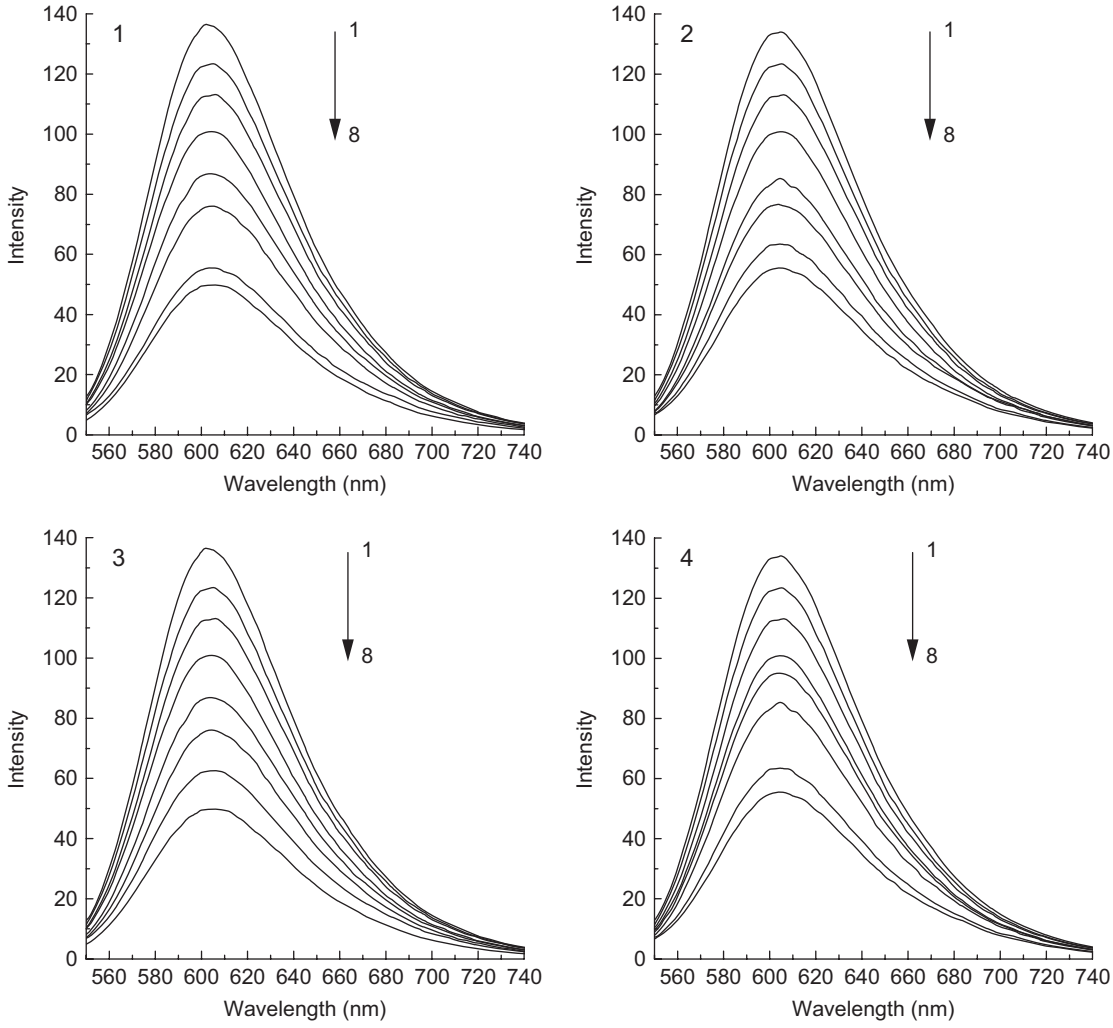

Figure 6. Fluorescence spectra of binding of EtBr to DNA in the absence (line 1) and presence (lines 2–8) of increasing amounts of complexes. λ_{ex} = 526 nm, C_{EtBr} = 1.0 μM, C_{DNA} = 5.1 μM, $C_{M(1-4)}$ (lines 2–8): 2.5, 5.0, 7.5, 12.5, 25, 37.5, 50 μM.

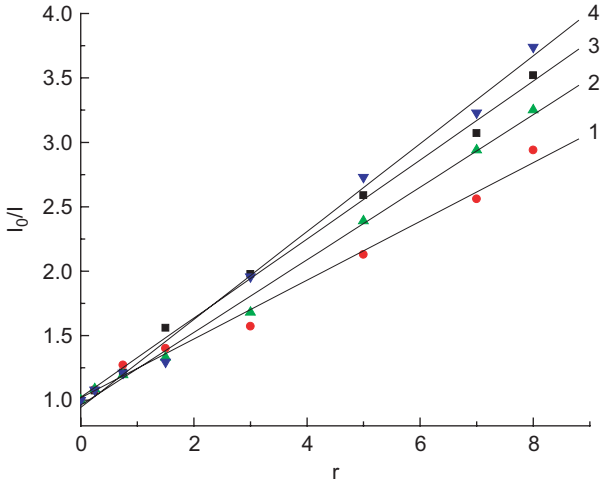

Figure 7. Stern–Volmer quenching plots of complexes 1, 2, 3, and 4 with values of slope 0.228 (1), 0.282 (2), 0.307 (3), and 0.341 (4).

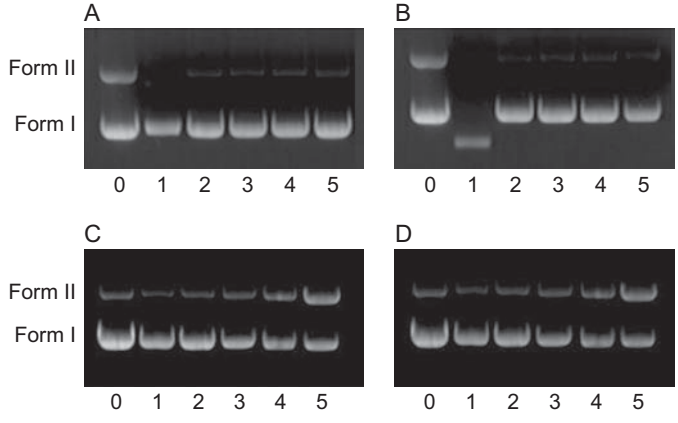

Figure 8. Cleavage of pBR322 DNA (10 μM) in the presence of complexes. Lane 0, DNA alone; lanes 1–5, in different concentrations of complex: 1, 3.5; 2, 7.0; 3, 14.0; 4, 21.0; 5, 28.0 μM. Quantitation % of Form II: a (0–5): 40.60, 0, 3.84, 3.11, 4.03, 3.99; b (0–5): 41.74, 0, 1.788, 2.82, 3.24, 2.57; c (0–5): 13.81, 7.38, 10.63, 19.58, 40.63, 90.01; d (0–5) 15.74, 9.92, 13.35, 23.91, 41.75, 90.84. a: complex 1, b: complex 2, c: complex 3, d: complex 4.

Table 3. Cytotoxicity of the complexes against selected human tumor cells after 72 h of incubation.

	In vitro activity (IC_{50} ± SD, μM)				
Tumor cells	Complex 1	Complex 2	Complex 3	Complex 4	Cisplatin
Hela	9.28 ± 1.92	8.71 ± 1.35	5.64 ± 0.97	4.37 ± 0.71	0.59 ± 0.11
Hep-G2	12.47 ± 2.14	10.69 ± 1.58	8.72 ± 1.76	6.24 ± 1.54	1.77 ± 0.27
KB	15.82 ± 2.43	12.39 ± 2.76	10.84 ± 1.24	8.15 ± 1.93	1.48 ± 0.35
AGZY-83a	17.24 ± 3.41	15.93 ± 2.71	13.42 ± 2.19	11.73 ± 2.46	2.13 ± 0.48

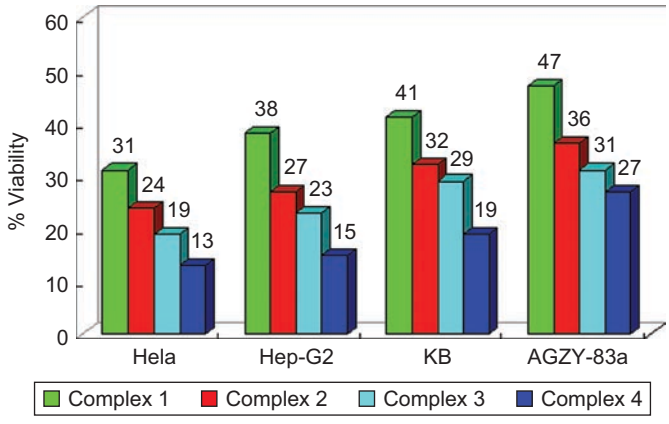

Figure 9. Effect of 3 μg/mL of complexes on breast cancer cell viability after 72 h of incubation. All determinations are expressed as percentage of control (untreated cells).

accordance with the classical Stern–Volmer equation[30]: $I_0/I = 1 + K_{sq}r$, where I_0 and I represent the fluorescence intensities in the absence and presence of the complex, respectively, and r is the concentration ratio of the complex to DNA. K_{sq} is a linear Stern–Volmer quenching constant dependent on the ratio of the bound concentration of EtBr to the concentration of DNA. The K_{sq} value is obtained as the slope of the I_0/I vs. r linear plot. The plots for quenching of DNA–EtBr fluorescence by the four complexes are given in Figure 7. From the insets in Figure 7, the K_{sq} values for the four complexes are, respectively, 0.228, 0.283, 0.307, and 0.341 ($K_{sq}4 > K_{sq}3 > K_{sq}2 > K_{sq}1$). Such a value of quenching constant suggests that the interaction of the complex with DNA is of moderate intercalation[31,32]. The data also indicate that the intercalation ability of the coordinated ligands varies as phen > bipy in this series of complexes[33]. In addition, the Pt(II) complexes have a better effect than Pd(II) on the fluorescence intensity of EtBr–DNA being quenched. Evidently, the outcome conforms to the order of complex 4 > complex 3 > complex 2 > complex 1. Thus, it can be confirmed that the reactions of the four intercalation complexes between the adjacent DNA base pairs have taken place[34].

Cleavage of pBR322 DNA by complexes

The ability of complexes to perform DNA cleavage is generally monitored by agarose gel electrophoresis, usually involving pUC19 plasmid DNA, pBR322 plasmid DNA, and pUC18 plasmid DNA[35–37]. The degree to which the four complexes could function as DNA-cleavage agents was measured using supercoiled pBR322 plasmid DNA as the aim. Four complexes, 1,2,3 and 4, were established to promote the cleavage of pBR322 plasmid DNA from supercoiled Form I to the nicked Form II (Figure 8). As shown in Figure 8, two clear bands were observed for the control, in which the metal complex was absent (lane 0). The complexes could induce cleavage of the plasmid DNA at the concentration of 3.5 μM. The amount of Form I of pBR322 DNA decreased gradually due to the concentration increase of the four complexes (lanes 1–5), whereas Form II increased. Also, the complexes showed different cleaving efficiencies for the plasmid DNA. Under comparable experimental conditions, Pt(II) complexes exhibited less effective DNA-cleavage activity than Pd(II) complexes. The different DNA-cleavage efficiencies of the complexes may be due to the different binding affinities of the complexes to DNA[20,22,38,39].

Cytotoxicity in vitro study

In vitro cytotoxicity tests of the four complexes using selected human tumor cell lines were carried out. The IC_{50} values are revealed in Table 3. In addition, Figure 9 shows the effect on cell growth after a period of 72 h of treatment with 3 μg/mL concentration. Among the complexes investigated here, complex 1 is the least cytotoxic in all four cell lines tested, while complex 4 is the most. The Pt(II) complexes were generally more active than Pd(II) conjugate analogs, especially against HeLa cells, which shows a high level of resistance against conventional chemotherapeutic agents (compound 1 is about 1/16 of cisplatin, compound 2: 1/15, compound 3: 1/10, compound 4: 1/7). A viability rate by day 3 to less than 50% of the control values was observed for the complexes. On the whole, the complexes were more effective in restraining the growth of HeLa than of the other lines, and showed a similar activity to cisplatin against the human tumor cell lines.

Acknowledgements

We gratefully acknowledge support of the National Natural Science Foundation of China (Nos. 20671064 and 20971090), Foundation of Educational Department of Liaoning Province (No. 20060679), Phenom Foundation of Liaoning colleges and universities (No. 2007R30), and Foundation of Liaoning Bai Qian Wan Talents Program (No. 2008921054). We thank Linda Li of Princeton University (USA) for reading and editing the manuscript.

***Declaration of interest*:** The authors report no conflicts of interest. The authors alone are responsible for the content and writing of the paper.

References

1. Liu YZ, Vinje J, Pacifico C, Natile G, Sletten E. Formation of adenine–n3/guanine–n7 cross-link in the reaction of trans-oriented platinum substrates with dinucleotides. J Am Chem Soc 2002;124:12854–62.
2. Reedijk J. The relevance of hydrogen bonding in the mechanism of action of platinum antitumor compounds. Inorg Chim Acta 1992;198:873–81.
3. Milacic V, Chen D, Ronconi L, Landis-Piwowar KR, Fregona D, Dou QP. A novel anticancer gold(iii) dithiocarbamate compound inhibits the activity of a purified 20s proteasome and 26s proteasome in human breast cancer cell cultures and xenografts. Cancer Res 2006;66:10478–86.
4. Sherman SE, Lippard SJ. Structural aspects of platinum anticancer drug interactions with DNA. Chem Rev 1987;87:1153–81.
5. Reedijk J, Appl P. The mechanism of action of platinum anti-tumor drugs. Pure Appl Chem 1987;59:181–6.
6. Miernicka M, Szulawska A, Czyz M, Lorenz I, Mayer P, Karwowski B, et al. Cytotoxic effect, differentiation, inhibition of growth and theoretical calculations of an N,N-donor ligand and its platinum(II), palladium(II) and copper(II) complexes. J Inorg Biochem 2008;102:157–65.
7. Zhao GH, Lin HK. Metal complexes with aromatic N-containing ligands as potential agents in cancer treatment. Chem Anticancer Agents 2005;5:137–47.
8. Yu SY, Fujita M, Yamaguchi K. A dimer-to-dimer metal–metal linear aggregate from a (μ-1,3-NO3)2 double-bridged cis-(2,2′-bipyridine)palladium(II) cofacial dimer. J Chem Soc Dalton Trans 2001:3415–16.
9. Suggs JW, Dube MJ, Nichols M. Organometallic photonucleases: a novel class of DNA-cleaving agents. J Chem Soc Chem Commun 1993:307–9.
10. Suggs JW, Higgins JD, Wagner RW, Millard JT. In: Metal–DNA Interactions. Washington, DC: American Chemical Society, 1989:Ch. 10.
11. Lempers EM, Rarilla A, Suh M, Kostic NM. in: T.D. Tullius, (Ed.), Book of Abstracts Division of Inorganic Chemistry, National Meeting Spring, No. 362, Washington, DC, American Chemical Society, 1991.
12. Mital R, Srivastava TS. Synthesis, characterization, and DNA binding studies of some mixed-ligand platinum(II) complexes of 1,10-phenanthroline and amino acids. J Inorg Biochem 1990;40:111–20.
13. Vital R, Srivastava TS, Parekh HK, Chitnis MP. Synthesis, characterization, DNA binding, and cytotoxic studies of some mixed-ligand palladium(II) and platinum(II) complexes of α-diimine and amino acids. J Inorg Biochem 1991;41:93–103.
14. Altomare A, Burla MC, Camalli M, Cascarano GL, Giacovazzo C, Guagliardi A, et al. A new tool for crystal structure determination and refinement. J Appl Crystallogr 1999;32:115–19.
15. Sheldrick GM. SHELXL-97, 97-2 Version, University of Göttingen, Germany, 1997.
16. Alley MC, Scudiero DA, Monks A, Hursey ML, Czerwinski MJ, Fine DL, et al. Feasibility of drug screening with panels of human tumor cell lines using a microculture tetrazolium assay. Cancer Res 1988;48:589–601.
17. Cummings SD, Eisenberg R. Luminescent platinum(II) complexes of quinoxaline-2,3-dithiolate. Inorg Chem 1995;34:2007–14.
18. Makedonas C, Mitsopoulou CA, Lahoz FJ, Balana AI.Synthesis, characterization, and crystal structure of the Pd(phen)(bdt) complex. A DFT and TDDFT study of its ground electronic and excited states compared to those of analogous complexes. Inorg Chem 2003;42:8853–65.
19. Gao EJ, Zhu MC, Yin HX, Liu L, Wu Q, Sun YG. Synthesis, characterization, interaction with DNA and cytotoxicity in vitro of dinuclear Pd(II) and Pt(II) complexes dibridged by 2,2′-azanediyldibenzoic acid. J Inorg Biochem 2008;102:1958–64.
20. Gao EJ, Wang KH, Gu XF, Yu Y, Sun YG, Zhang WZ, et al. A novel binuclear palladium complex with benzothiazole-2-thiolate: synthesis, crystal structure and interaction with DNA. J Inorg Biochem 2007;101:1404–9.
21. Janiak C. A critical account on π–π stacking in metal complexes with aromatic nitrogen-containing ligands. J Chem Soc Dalton Trans 2000;24:3885–96.
22. Zhang QL, Liu JG, Liu JZ, Li H, Yang Y, Xu H, et al. Effect of intramolecular hydrogen-bond on the DNA-binding and photocleavage properties of polypyridyl cobalt(III) complexes. Inorg Chim Acta 2002;33:934–40.
23. Zhang QL, Liu JG, Chao H, Xue GQ, Ji LN. DNA-binding and photocleavage studies of cobalt(III) polypyridyl complexes: [Co(phen)2IP]3+ and [Co(phen)2PIP]3+. J Inorg Biochem 2001;83:49–55.
24. Zou XH, Ye BH, Li H, Liu JG, Xiong Y, Ji LN. Mono- and bi-nuclear ruthenium(II) complexes containing a new asymmetric ligand 3-(pyrazin-2-yl)-as-[triazino5,6-f]1,10-phenanthroline: synthesis, characterization and DNA-binding properties. J Chem Soc Dalton Trans 1999;9:1423–8.
25. He XF, Wang L, Chen H, Xu L, Ji LN. Synthesis, characterization and DNA binding study of Co(III) polypyridyl mixed-ligand complexes. Polyhedron 1998;17:3161–6.
26. Wolfe A, Shimer GH, Meehan T. Polycyclic aromatic hydrocarbons physically intercalate into duplex regions of denatured DNA. Biochemistry 1987;26:6392–6.
27. Strothkamp KG, Strothkamp RE. Fluorescence measurements of ethidium binding to DNA. J Chem Educ 1994;71:77–9.
28. Yang BS, Feng JY, Li YQ, Gao F, Zhao YQ, Wang JL. Spectral studies on aluminum ion binding to the ligands with phenolic group(s): implications for the differences between N- and C-terminal binding sites of human serum apotransferrin. J Inorg Biochem 2003;96:416–24.
29. Baguley BC, Bret ML. Quenching of DNA-ethidium fluorescence by amsacrine and other antitumor agents: a possible electron-transfer effect. Biochemistry 1984;23:937–43.
30. Lakowicz JR, Weber G. Quenching of fluorescence by oxygen. Probe for structural fluctuations in macromolecules. Biochemistry 1973;12:4161–70.
31. Baguley BC, Bret ML. Quenching of DNA-ethidium fluorescence by amsacrine and other antitumor agents: a possible electron-transfer effect. Biochemistry 1984;23:937–43.
32. Liu J, Zhang TX, Lu TB, Qu LH, Zhou H, Zhang QL, et al. DNA-binding and cleavage studies of macrocyclic copper(II) complexes. J Inorg Biochem 2002;91:269–76.
33. Ghosh S, Barve AC, Kumbhar AA, Kumbhar AS, Puranik VG, Datar PA, et al. Synthesis, characterization, X-ray structure and DNA photocleavage by cis-dichloro bis(diimine) Co(III) complexes. J Inorg Biochem 2006;100:331–43.
34. Arakawa H, Ahmad R, Naoui M, Tajmir-Riahi HA. A comparative study of calf thymus DNA binding to Cr(III) and Cr(VI) ions. Evidence for the guanine N-7-chromium-phosphate chelate formation. J Biol Chem 2000;274:10150–3.
35. Moreno RGM, Alipázaga MV, Gomes OF, Linares E, Medeiros MHG, Coichev N. DNA damage and 2′-deoxyguanosine oxidation induced by S(IV) autoxidation catalyzed by copper(II) tetraglycine complexes: synergistic effect of a second metal ion. J Inorg Biochem 2007;101:866–75.
36. Macías B, Villa MV, Gómez B, Borrás J, Alzuet G, González-Alvarez M, et al. DNA interaction of new copper(II) complexes with sulfonamides as ligands. J Inorg Biochem 2007;101:444–51.
37. Ghosh S, Barve AC, Kumbhar AA, Kumbhar AS, Puranik VG, Datar PA, et al. Synthesis, characterization, X-ray structure and DNA photocleavage by cis-dichloro bis(diimine) Co(III) complexes. J Inorg Biochem 2006;100:331–43.
38. Wang XL, Chao H, Li H, Hong XL, Liu YJ, Tan LF, et al. DNA interactions of cobalt(III) mixed-polypyridyl complexes containing asymmetric ligands. J Inorg Biochem 2004;98:1143–50.
39. Qian J, Gu W, Liu H, Gao FX, Feng L, Yan SP, et al. The first dinuclear copper(II) and zinc(II) complexes containing novel Bis-TACN: syntheses, structures, and DNA cleavage activities. Dalton Trans 2007;10:1060–6.